

# miR-124-3p Regulates FGF2–EGFR Pathway to Overcome Pemetrexed Resistance in Lung Adenocarcinoma Cells by Targeting MGAT5

This article was published in the following Dove Press journal:  
*Cancer Management and Research*

Jundong Cai<sup>1</sup>  
Jiuning Huang<sup>1,2</sup>  
Wulong Wang<sup>1</sup>  
Jing Zeng<sup>1</sup>  
Ping Wang<sup>1</sup>

<sup>1</sup>Department of Radiotherapy, Tianjin Medical University Cancer Institute and Hospital, National Clinical Research Center for Cancer, Tianjin Key Laboratory of Cancer Prevention and Therapy, Tianjin's Clinical Research Center for Cancer, Tianjin 300000, People's Republic of China; <sup>2</sup>Department of Radiotherapy, Yantai Affiliated Hospital of Binzhou Medical University, Yantai 264000, Shandong, People's Republic of China

**Objective:** To investigate whether miR-124-3p regulates the fibroblast growth factor 2 (FGF2)–epidermal growth factor receptor (EGFR) pathway by targeting MGAT5 to affect the pemetrexed resistance in lung adenocarcinoma cells.

**Methods:** PC9-MTA and H1993-MTA anti-pemetrexed lung adenocarcinoma cell lines were constructed. The cell viability of anti-pemetrexed and parent lung adenocarcinoma cells was analyzed using MTS assay and reverse transcription PCR to determine the expression of miR-124-3p. CCK8 assay, colony formation assay, and flow cytometry were used to determine cells' proliferation and apoptosis. FGF2–EGFR signaling pathway-related proteins and MGAT5 protein expression were quantified by Western blotting. The target relationship between miR-124-3p and MGAT5 was verified by double luciferase assay. A nude mouse model with a transplanted tumor was established using the anti-pemetrexed lung adenocarcinoma cells. Tumor volume and weight were determined, and the apoptosis of tumor cells was observed.

**Results:** The half-maximal inhibitory concentration of pemetrexed in anti-pemetrexed lung adenocarcinoma cells was higher than that in parent lung adenocarcinoma cells, and the expression of miR-124-3p in the anti-pemetrexed cells was lower than that of the parent cells. In the miR-124-3p overexpression group, MGAT5 silencing group, and miR-124-3p +MGAT5 overexpression group, compared with the control group, the proliferation ability of cells and tumors was markedly reduced; their apoptosis rates were increased significantly; expression levels of FGF2 and p-EGFR/EGFR were decreased; and the growth rate and tumor volume and mass were reduced; however, the opposite results were obtained in the miR-124-3p silencing group ( $p < 0.05$ ).

**Conclusion:** miR-124-3p may inhibit the FGF2–EGFR pathway by targeting MGAT5 to decrease pemetrexed resistance in lung adenocarcinoma cells.

**Keywords:** miR-124-3p, MGAT5, FGF2-EGFR pathway, lung adenocarcinoma

Correspondence: Ping Wang  
Department of Radiotherapy, Tianjin Medical University Cancer Institute and Hospital, National Clinical Research Center for Cancer, Tianjin Key Laboratory of Cancer Prevention and Therapy, Tianjin's Clinical Research Center for Cancer, Huanhu Xi Road, Tiyan Bei, Hexi District, Tianjin 300000, People's Republic of China  
Tel +86-18622221112  
Email pingwang2020@163.com

## Introduction

Lung cancer is one of the leading causes of death among all malignant cancers, endangering human health and life. Lung adenocarcinoma, a subtype of non-small-cell lung cancer (NSCLC), is the most common histological type of lung cancer, representing approximately 40% of NSCLC cases. Its incidence has increased in recent years, and it causes nearly 200 million deaths worldwide each year.<sup>1–3</sup> Despite some progress in the treatment of lung cancers in recent decades, the prognosis of patients with lung adenocarcinoma is not optimistic, and the overall

survival rate is less than 15%.<sup>4</sup> Many patients are in advanced stages at diagnosis and cannot be treated with surgery; thus, chemotherapy has become the first choice of treatment. Other treatment options include radiotherapy, targeted therapies, and immunotherapy. Platinum-based chemotherapy is the current first-line treatment,<sup>5</sup> but its efficacy is limited, with unsatisfactory improvements in 1-year survival. Resistance to chemotherapy drugs, which occurs in most patients and eventually leads to treatment failure, is the main limiting factor in improving the efficacy of chemotherapy.<sup>6</sup>

Pemetrexed is a new type of folate metabolism antagonist that represents a new generation of anti-tumor drugs for the treatment of lung adenocarcinoma. Alone or combined with other chemotherapy drugs, it has had an important role in first-line, second-line, and maintenance therapy in recent years,<sup>7,8</sup> but its effects are again limited by drug resistance.<sup>9</sup> This underlines the importance of studying drug resistance mechanisms in lung adenocarcinoma chemotherapy.

In recent years, researchers have noted the correlation between abnormal molecular expression and tumor formation. For example, thymidine nucleotide synthetase, epidermal growth factor receptor (EGFR), and other target genes have been identified, and various targeted drugs have been developed; however, although this has increased the 5-year survival rate of patients with lung adenocarcinoma, the overall survival rate remains relatively low.<sup>10,11</sup> Therefore, finding potential new gene targets will help to overcome drug resistance in lung adenocarcinoma cells, thereby improving the prognosis of patients.

MicroRNAs (miRNAs) are small non-coding molecule RNAs that exist widely in eukaryotes and are about 18–25 nucleotides in length. In the past decade, the role of microRNAs in tumors has been a focus of research, showing that they are pivotal in post-transcriptional regulation. miRNAs can directly regulate tumor proliferation by combining with the 3' untranslated region (UTR) of the target gene's mRNA.<sup>12</sup> miR-124 is a highly conserved miRNA, which has been shown to be associated with drug resistance in various tumors, including gastric cancer,<sup>13</sup> breast cancer,<sup>14</sup> and thyroid carcinoma.<sup>15</sup> N-acetylglucosaminyltransferase V (MGAT5), an important N-glycan-processing enzyme distributed in the Golgi apparatus, affects the tumor metastasis of cells.<sup>16</sup> Wang and colleagues found that MGAT5 was a direct target gene of miR-124-3p in breast cancer, and that restoration of MGAT5 attenuated the inhibitory effects of miR-124-3p on breast cancer proliferation and

metastasis.<sup>16</sup> However, there have been few studies on the role and function of miR-124-3p in lung adenocarcinoma and its effects on drug resistance.

In this article, we constructed anti-pemetrexed lung adenocarcinoma cell lines (PC9-MTA, H1993-MTA), and established a nude mouse model with transplanted tumors using these cells, to explore whether miR-124-3p could regulate the fibroblast growth factor 2 (FGF2)–EGFR pathway by targeting MGAT5 to suppress the growth of lung adenocarcinoma cells.

## Methods

### Cell Culture and Construction of Anti-Pemetrexed Lung Adenocarcinoma Cell Lines PC9-MTA, and H1993-MTA

Human lung adenocarcinoma cell lines PC9 (mutant EGFR, EGFR-DelE746\_A750, BIV10058, BioInnovatise) and H1993 (wild type) were purchased from BNCC (BNCC331211) and cultured in RPMI-1640 complete medium containing 10% fetal bovine serum and 1% penicillin-streptomycin (HyClone, USA) in a constant-temperature incubator (Thermo, USA). Logarithmic-phase cells were selected for use in experiments.

Using a high-concentration repeated intermittent induction method, PC9 and H1993 lung adenocarcinoma cells were cultured in RPMI-1640 medium containing  $10^{-5}$  mol/L pemetrexed (Shandong Qilu Pharmaceutical Company). After continuous treatment for 24 h, the culture medium was replaced with fresh medium with no drug. Dead sensitive cells were removed. When the survival cells grew stably and the fusion degree reached 70–80%, cells were treated again with the same dose. The half-maximal inhibitory concentration ( $IC_{50}$ ) was detected repeatedly until it was five times that before induction, indicating that acquired drug resistance had been successfully induced.

### 3-(4,5-Dimethylthiazol-2-Yl)-5-(3-Carboxymethoxyphenyl)-2-(4-Sulfophenyl)-2H-Tetrazolium (MTS) Cell Proliferation Colorimetric Assay

Cells were divided into a blank group and pemetrexed groups of different concentrations (100, 10, 1, and 0  $\mu\text{mol/L}$ ), where the 0  $\mu\text{mol/L}$  group was the control. Cells in the logarithmic growth phase were digested using 0.25% pancreatin and plated in a 96-well plate at a concentration of 5000 cells/

100  $\mu$ L. The medium was changed the next day. After 48 h of drug treatment, 20  $\mu$ L of MTS reagent (purchased from Promega, USA) was poured into each well, followed by incubation for 3 h at 37°C. The optical density (OD) of each well (OD = 490 nm) was read using an enzyme-labeled instrument. The cell survival rate was calculated as follows: (OD<sub>490</sub> of experimental group – OD<sub>490</sub> of blank group)/OD<sub>490</sub> of control group – OD<sub>490</sub> of blank group)  $\times$  100%. A drug dose-response curve was constructed, and the IC<sub>50</sub> and resistance index (RI) were calculated as follows: RI = IC<sub>50</sub> (resistant cell)/IC<sub>50</sub> (parental cell).

Cells in the logarithmic growth phase were collected and seeded in a 96-well plate at 5000 cells/100  $\mu$ L and cultured for 24 h, and the morphology of cells was observed using an inverted phase contrast microscope (IMT-2, Olympus).

## Reverse Transcription Polymerase Chain Reaction (RT-PCR)

Detection of miR-124-3p expression was performed by RT-PCR. The total RNA of cells in each group was extracted by the TRIzol method. cDNA was reverse transcribed. Real-time fluorescence quantitative PCR was used to verify the mRNA expression levels of miR-124-3p and MGAT5 in cells. Reaction conditions were as follows: pre-denaturing at 95°C for 15 min, 95°C for 5 s, annealing at 64°C for 30 s, 40 cycles. Data were processed and calculated based on the  $2^{-\Delta\Delta C_t}$  method, and the relative expression levels were evaluated using U6 and  $\beta$ -actin mRNAs as internal references. Primer sequences (Sangon Biotech (Shanghai) Co., Ltd.) are shown in Table 1.

## Cell Transfection and Grouping

One day before transfection, anti-pemetrexed lung adenocarcinoma cells (PC9-MTA, H1993-MTA) were passaged

separately, cultured in six-well plates, and transfected with lentivirus.<sup>17</sup> The lentiviral particles were constructed by Shanghai GeneChem Co., Ltd. Cells were grouped as follows: control group (cells were not treated); miR-124-3p overexpression negative control group (mimic-NC, cells transfected with 100 nM of miR-124-3p mimic negative control); miR-124-3p overexpression group (miR-124-3p, cells transfected with 100 nM of miR-124-3p mimic); miR-124-3p silencing negative control group<sup>18</sup> (siRNA-NC, cells transfected with 100 nM of miR-124-3p silencing negative control); miR-124-3p silencing group (si-miR, cells transfected with 100 nM of miR-124-3p short interfering RNA (siRNA)). RT-PCR was used to detect the expression of miR-124-3p mRNA in cells 72 h after transfection. The sequences are as follows.

mimic-NC 5'-UUCUCCGAACGUCACGUTT-3';

miR-124-3p mimic 5'-UAAGGC ACGCGGUGAAU GCC-3';

miR-124-3p siRNA 5'-CGUGUUCACAGCGGACC UU GAU-3';

siRNA-NC 5'-CCGUACUUCGCUAGAUA-3'.

## Cell Counting Kit-8 (CCK8) Assays to Detect Cell Proliferation

Cells of each group were plated in a 96-well plate at a density of  $2 \times 10^4$  cells/mL, 100  $\mu$ L per well, and placed in a 37°C, 5% CO<sub>2</sub> incubator. After culture for 24 h, CCK-8 solution (Dojindo Laboratories, Japan) was added to each well, 10  $\mu$ L per well, evenly mixed, and cultured for 4 h. The absorbance (OD) of each well was measured at 450 nm with a microplate reader zeroed by a blank well.

## Colony Formation Assay

A single-cell suspension was prepared, and cells were plated in a six-well plate, 500 cells per well. After 2–3 weeks, visible colonies appeared on the plate, and the culture was terminated. The culture medium in the wells was discarded, methanol was added for fixation, and 1 mL of Giemsa working solution was added to each well for dyeing for 30 min. The dye was washed off slowly with running water. The plate was dried in air and imaged using a camera.

## Flow Cytometry

Cells were cultured for 24 h after treatment, collected, resuspended in precooled phosphate-buffered saline (4°C), and washed twice. Subsequently, 1 $\times$  binding buffer was added to resuspend the cells. Then, 5  $\mu$ L of Annexin

**Table 1** Primer Sequences

Gene	Sequence
miR-124-3p	Forward: 5'- CGACGTAAGGCACGCG –3' Reverse: 5'- CAGTGCAGGGTCCGAGGTAT –3'
U6	Forward: 5'- GACCTCTATGCCAACACAGT –3' Reverse: 5'- AGTACTTGCGCTCAGGAGGA –3'
MGAT5	Forward: 5'- AGGGCCATCCTGGGTTCATTA –3' Reverse: 5'- AAAGTCTGCTGCGGGTTCAGATTC –3'
$\beta$ -actin	Forward: 5'- CTGGTGCCTGGGGCG –3' Reverse: 5'- AGCCTCGCCTTTGCCGA –3'

V-FITC was added, mixed, and incubated at room temperature for 15 min in the dark. Next, 5  $\mu$ L of propidium iodide dye was added 5 min before the test, followed by 200  $\mu$ L of 1  $\times$  binding buffer. Finally, the samples were measured using a flow cytometer (Beckman Coulter, Brea, CA, USA) and the results were evaluated with the Cell Quest software (BD Bioscience, San Diego, CA).

## Western Blotting

Western blotting was used to detect expression of FGF2–EGFR signaling pathway-related proteins and MGAT5 protein. Tumor tissues were taken from the freezer at  $-80^{\circ}\text{C}$ , and the total protein of tissues and cells was extracted. The BCA method was used to measure the concentration of protein. The protein of each group was adjusted to ensure equal concentrations, and an appropriate amount of buffer solution was added, followed by boiling for 5 min. Proteins were separated by electrophoresis with a 5–12% separation gel and 5% concentrated gel, then transferred to membrane and finally blocked using 5% skimmed milk powder at room temperature for 2 h. The membrane was incubated with diluted primary antibodies FGF2 (1:1000, DF6038, Affinity), p-EGFR (1:1000, AF3042, Affinity), EGFR (1:1000, AF6042, Affinity), MGAT5 (1:500, orb100294, Biorbyt, Cambridge, UK), and GAPDH (1:1000, ET1702, HUABIO) polyclonal antibody overnight at  $4^{\circ}\text{C}$ , followed by incubation with diluted secondary antibody horseradish peroxidase (HRP)-labeled goat anti-rabbit IgG (1:500, orb338796, Biorbyt, Cambridge, UK) at room temperature for 2 h. Finally, electrochemiluminescence was used to expose the protein bands. The gray values of the obtained bands were analyzed with Image J (National Institutes of Health, version 6).

## Dual-Luciferase Reporter Assay System

Wild-type and mutant 3' UTRs of MGAT5 were, respectively, amplified in a pGL3/luciferase vector (Promega, Madison, WI, USA) and cloned downstream of the luciferase gene. Forty-eight hours after transfection, the luciferase activity of 293T cells was detected using a dual-luciferase reporter system (Promega)<sup>16</sup> according to the instructions.

## PCR to Determine Whether miR-124-3p Regulates FGF2–EGFR Pathway by Targeting MGAT5

The cells were grouped as follows: (a) control group (Control); (b) miR-124-3p overexpression group (miR-124-3p); (c) MGAT5 silencing group (sh-MGAT5, cells

transfected with 100 nM of MGAT5 siRNA<sup>19</sup>); (d) MGAT5 silencing negative control group (sh-NC): cells transfected with 100 nM of MGAT5 siRNA negative control; (e) miR-124-3p overexpression + MGAT5 overexpression group (miR+MGAT5): cells simultaneously transfected with of 100 nM of miR-124-3p mimic and 100 nM of MGAT5 mimic; (f) miR-124-3p overexpression + MGAT5 overexpression negative control group (miR+M-NC): cells simultaneously transfected with 100 nM of miR-124-3p mimic and 100 nM of MGAT5 mimic negative control. RT-PCR was used to determine the expression of MGAT5 in cells, and the above indicators were tested again.

## Construction and Grouping of Transplanted Tumors in Nude Mice

Specific-pathogen-free grade Balb/c male nude mice (4 weeks old, weighing 16–18 g, n = 48) were purchased from the Beijing Vital River Laboratory Animal Technology Co., Ltd. (No. SCXK (Jing) 20160006; Beijing, China). They were kept in a sterile independent ventilation cage in a room with an air laminar-flow purifying system. Indoor air was disinfected by ultraviolet light. A constant temperature ( $23\text{--}25^{\circ}\text{C}$ ) and relative humidity (60–80%) were maintained. The feed, water, and bedding materials were sterilized for use in the experiment. Cushion material was replaced every other day. The animal experiments followed the National Institutes of Health laboratory animal care and usage guidelines (No. 85–23, revised 1996) and were approved by the committee of Tianjin Medical University Cancer Institute and Hospital.

Cells were collected, and the cell concentration of each group was adjusted to  $5 \times 10^7$  cells/mL.<sup>17</sup> Then, 0.1 mL of cell suspension was inoculated into the soft skin of the right forelimbs of the nude mice. Forty eight nude mice were randomly divided into four groups (n=12): control group, miR-124-3p overexpression group (miR-124-3p), MGAT5 silencing group (sh-MGAT5), and miR-124-3p overexpression + MGAT5 overexpression group (miR+MGAT5).

## Tumor Volume Calculation

The long diameter (L) and short diameter (W) of tumors were measured using a Vernier caliper every 7 days, and the volume of the tumor was calculated as follows: tumor volume (V) =  $(L \times W^2)/2$ . Twenty-eight days after vaccination, the nude mice were anesthetized by an intraperitoneal injection of 0.6% pentobarbital sodium (40 mg/kg) and

then sacrificed by neck removal. Tumor tissues were removed and weighed. Part of the tumor tissue was fixed in 4% paraformaldehyde, then embedded in paraffin and stored in liquid nitrogen.

## Immunohistochemical Detection of Ki67 Expression in Tumor Tissue

After the tumor tissue had been embedded and sectioned conventionally, it was baked, dewaxed in xylene, and hydrated sequentially using a gradient ethanol solution. Subsequently, the slices were inactivated for 20 min in 3% H<sub>2</sub>O<sub>2</sub> methanol solution, hot-repaired with high-temperature antigen in citrate buffer (pH 6.0) for 10 min, and blocked with 5% bovine serum albumin for 20 min. Rabbit anti-human Ki67 (1:200, AF5208, Affinity) polyclonal antibody was added to the slices and reacted overnight at 4°C. After rewarming, they were incubated with the second antibody, goat anti-rabbit IgG labeled with HRP (1:1000, ABIN101988, antibodies online, Germany) and then stained with DAB, re-stained, dehydrated, and sealed. Cells were observed and photographed under an optical microscope (Olympus, Japan, ×400) and counted using the Aperio ImageScope 11.1 software. The results are expressed as the percentage of positive cells (%).

## TUNEL Detection of Tumor Cell Apoptosis

Slices (4 μm in thickness) were dewaxed in conventional xylene and then dehydrated with gradient ethanol. An apoptosis detection kit (T2190, Solarbio) was used to quantitatively detect apoptosis. Five fields of view were randomly chosen under an optical microscope (×400, BX50/Olympus Co., Ltd., Japan). If cells were brownish or brownish yellow and also had morphological characteristics of apoptotic cells, they were deemed to be apoptotic. The apoptotic index (AI) was calculated to represent the degree of apoptosis:  $AI = (\text{number of apoptotic positive cells} / \text{number of total cells}) \times 100\%$ .

## Statistical Analyses

All data were analyzed using the statistical analysis software SPSS 20.0. Results are presented as mean ± standard deviation. *t*-test was used for analysis of differences between two groups. Differences among multiple groups were calculated by one-way analysis of variance, and

Dunnett's test was used for subsequent analysis.  $p < 0.05$  was considered statistically significant.

## Results

### Characteristics of Anti-Pemetrexed and Parent Lung Adenocarcinoma Cells

As the concentration of pemetrexed was increased, the activity of cells in each group gradually decreased (Figure 1A). The cell viabilities of PC9-MTA and H1993-MTA cells were clearly higher than those of PC-9 and H1993 cells, respectively ( $p < 0.05$ ). IC<sub>50</sub> values for cells in each group were calculated (Figure 1B); those of PC9-MTA and H1993-MTA cells were significantly higher than those of PC-9 and H1993 cells, respectively ( $p < 0.05$ ). The RI of PC9-MTA cells was 75.18, and that of H1993-MTA cells was 73.60. The morphological changes of cells are shown in Figure 1C. There were no visible morphological differences between PC9 and PC9-MTA cells. After acquiring resistance to pemetrexed, H1993 cells changed from classic epithelial morphology to fusiform morphology. The expression of miR-124-3p in different cells was analyzed by RT-PCR (Figure 1D). The expression of miR-124-3p in PC9-MTA cells was significantly lower than that in PC9 cells, and the expression of miR-124-3p in H1993-MTA cells was also lower than that in H1993 cells ( $p < 0.05$ ).

### Effects of miR-124-3p Expression on the Biological Behavior of Anti-Pemetrexed Cells

In order to study the role of miR-124-3p in PC9-MTA and H1993-MTA cells, different expression levels of miR-124-3p were established using a miR-124-3p mimic and siRNA. The expression of miR-124-3p was measured in each group by RT-PCR (Figure 2A). The expression of miR-124-3p in miR-124-3p group was clearly higher than in the control group ( $p < 0.05$ ), and the expression of miR-124-3p in si-miR group was significantly lower than in the control group ( $p < 0.05$ ). Cell viability was analyzed by CCK-8 (Figure 2B) and colony formation assay (Figure 2C). Cell proliferation ability (Figure 2B) and colony numbers (Figure 2C) were markedly inhibited in the miR-124-3p group compared with the control group ( $p < 0.05$ ), whereas they were increased in the si-miR group compared with the control group ( $p < 0.05$ ). Furthermore, the apoptosis rate in each group was measured by flow cytometry (Figure 2D). Compared with the control group, the apoptosis rate in the

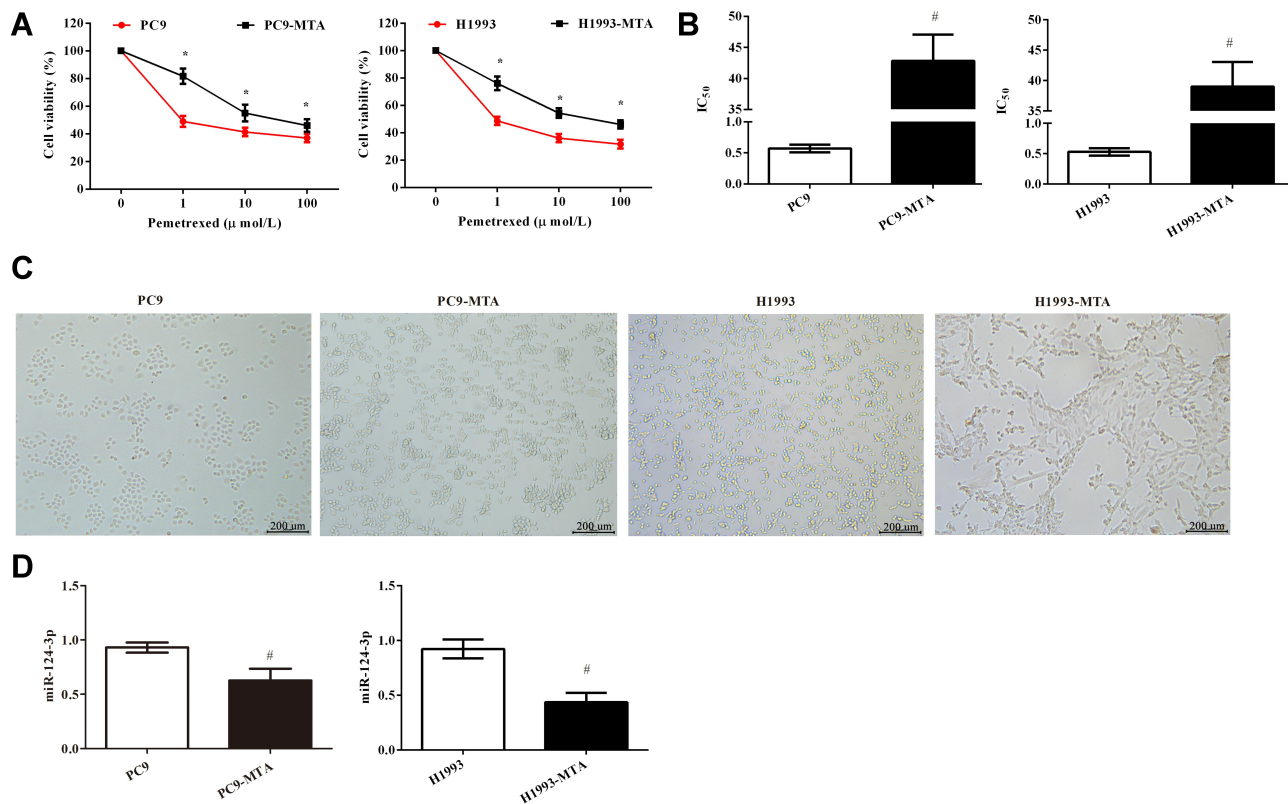


**Figure 1** Characteristics of anti-pemetrexed (PC9-MTA and H1993-MTA) and parent (PC9 and H1993) lung adenocarcinoma cells. **(A)** MTS was used to analyze cell viability. **(B)** IC<sub>50</sub> values for lung adenocarcinoma cells. **(C)** Morphological observation of anti-pemetrexed and parent lung adenocarcinoma cells. **(D)** RT-PCR was used to analyze the expression of miR-124-3p in lung adenocarcinoma cells. \* $p < 0.05$  compared with PC9 cells; # $p < 0.05$  compared with H1993 cells.

miR-124-3p group was significantly increased, and that of the si-miR group was significantly reduced ( $p < 0.05$ ).

## Effects of miR-124-3p on Expression of FGF2–EGFR Signaling Pathway-Related Proteins in Anti-Pemetrexed Cells

The expression of FGF2–EGFR signaling-related proteins was analyzed using Western blotting (Figure 3). As shown in the figure, the tendency of expression of FGF2 and p-EGFR/EGFR was similar in PC9-MTA and H1993-MTA cells. Compared with the control group, the expression levels of FGF2 and p-EGFR/EGFR in the miR-124-3p group were significantly decreased, whereas those in the si-miR group were increased ( $p < 0.05$ ). The expression of EGF2 and p-EGFR/EGFR in the si-miR group was increased compared with that in the miR-124-3p group ( $p < 0.05$ ).

## Dual-Luciferase Reporter Assay System

The expression of MAGT5 was analyzed using Western blotting in each group (Figure 4A and B). In PC9-MTA cells (Figure 4A), compared with the control group, the

expression of MAGT5 protein in miR-124-3p group was significantly reduced, whereas it was increased in the si-miR group ( $p < 0.05$ ). A similar tendency in the expression of MAGT5 was found in H1993-MTA cells (Figure 4B). In order to study the relationship between miR-124-3p and MAGT5 in anti-pemetrexed cells, MAGT5 was predicted as a target gene of miR-124-3p using TargetScan (Figure 4C), and a dual-luciferase reporter system was used to confirm miR-124-3p targets MAGT5 (Figure 4D). The results showed that the miR-124-3p mimic could decrease luciferase activity when transfected with wild-type MAGT5 but not with mutant MAGT5 ( $p < 0.05$ ).

## Effect of miR-124-3p Targeting MAGT5 on the Biological Behavior of Anti-Pemetrexed Cells

In addition, the PC9-MTA and H1993-MTA cells were further transfected with MAGT5 siRNA and MAGT5 mimic to study how miR-124-3p inhibits cell proliferation by targeting MAGT5. The expression of MAGT5 mRNA

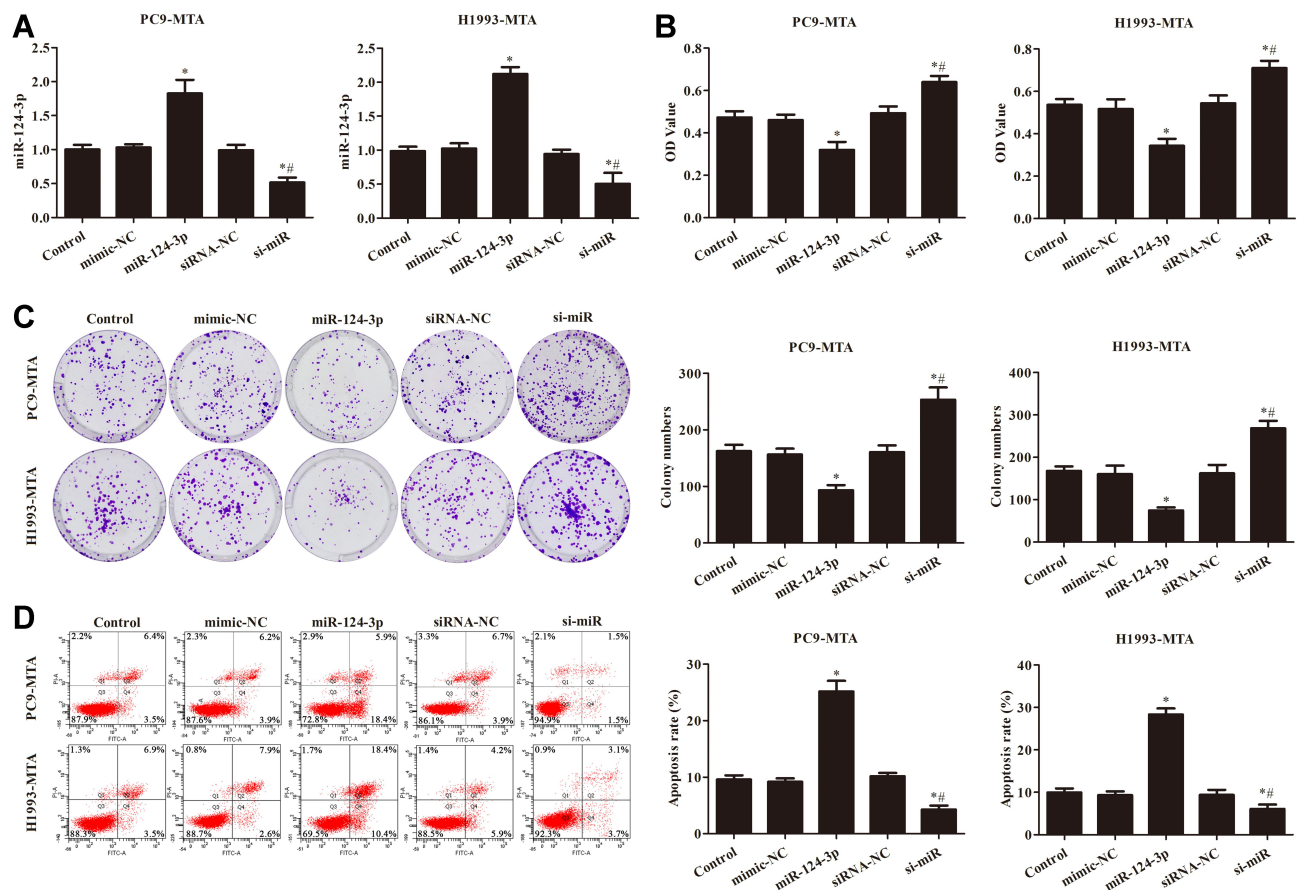


**Figure 2** Effects of differential miR-124-3p expression on the biological behavior of anti-pemetrexed cells. **(A)** RT-PCR was used to detect the expression of miR-124-3p in each group. **(B)** CCK8 assay was used to detect cell viability in each group. **(C)** Colony formation experiments were used to analyze cell proliferation. **(D)** Flow cytometry was used to detect cell apoptosis in each group. \* $p < 0.05$  compared with control group; \*\* $p < 0.05$  compared with miR-124-3p group.

**Abbreviations:** mimic-NC, miR-124-3p overexpression negative control group; miR-124-3p, miR-124-3p overexpression group; siRNA-NC, miR-124-3p silencing negative control group; si-miR, miR-124-3p silencing group.

in each group of PC9-MTA and H1993-MTA cells was measured by RT-PCR (Figure 5A). Compared with the control group, the expression of MGAT5 was clearly reduced in the sh-MGAT5 group ( $p < 0.05$ ). Compared with the miR-124-3p group, the expression of MGAT5 was significantly increased in the miR+MGAT5 group ( $p < 0.05$ ). Proliferation ability was analyzed by CCK-8 (Figure 5B) and colony formation assays (Figure 5C). Cell viability (Figure 5B) and colony numbers were significantly reduced in the sh-MGAT5 group compared with the control group ( $p < 0.05$ ); however, they were significantly increased in the miR+MGAT5 group compared with the miR-124-3p group ( $p < 0.05$ ). The apoptosis rate in each group was analyzed by flow cytometry (Figure 5D). The apoptosis rate was significantly increased in the MGAT5 group compared with the control group ( $p < 0.05$ ) but decreased in the miR+MGAT5 group compared with the miR-124-3p group ( $p < 0.05$ ).

## Effects of miR-124-3p Targeting MGAT5 on the Expression of FGF2–EGFR Signaling Pathway-Related Proteins in Anti-Pemetrexed Cells

The expression of FGF2–EGFR signaling-related proteins was analyzed using Western blotting (Figure 6). According to the results, the expression levels of EGF2 and p-EGFR/EGFR in the sh-MGAT5 group were lower than those in the control group ( $p < 0.05$ ). Compared with the miR-124-3p group, the expression levels of FGF2 and p-EGFR/EGFR in the miR+MGAT5 group were significantly increased ( $p < 0.05$ ).

## Effects of miR-124-3p Targeting MGAT5 on the Growth of Transplanted Tumors in Nude Mice

Tumors were transplanted into nude mice to confirm that miR-124-3p targeting of MGAT5 inhibited the anti-pemetrexed

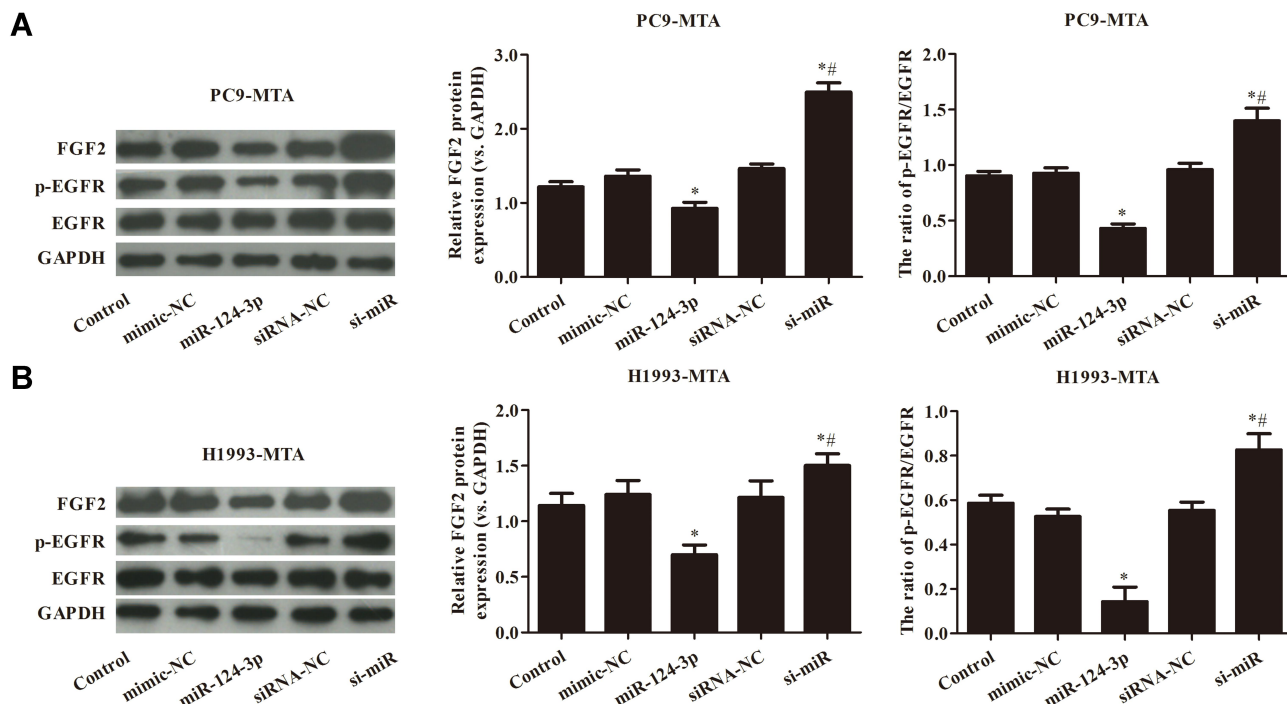


**Figure 3** Effects of differential miR-124-3p expression on the expression of FGF2–EGFR signaling pathway-related proteins in PC9-MTA cells (A) and H1993-MTA cells (B). \* $p < 0.05$  compared with control group; # $p < 0.05$  compared with miR-124-3p group.

**Abbreviations:** mimic-NC, miR-124-3p overexpression negative control group; miR-124-3p, miR-124-3p overexpression group; siRNA-NC, miR-124-3p silencing negative control group; si-miR, miR-124-3p silencing group.

lung adenocarcinoma cells. As shown in Figure 7A–C, tumor volumes and weights were measured. Compared with the control group, tumor growth was suppressed in the miR-124-3p and sh-MGAT5 groups ( $p < 0.05$ ). However, overexpression of MGAT5 weakened the effects of miR-124-3p ( $p < 0.05$ ). In addition, the expression of Ki-67 in tumor tissues of each group was analyzed by immunohistochemical detection (Figure 7D). The percentages of Ki67-positive cells in the tumor tissues of the miR-124-3p and sh-MGAT5 groups were distinctly reduced compared with the control group ( $p < 0.05$ ), and the percentage of Ki67-positive cells in tumor tissues of the miR +MGAT5 group was increased markedly compared with the miR-124-3p group ( $p < 0.05$ ).

### Effects of miR-124-3p Targeting MGAT5 on Apoptosis of Transplanted Tumors in Nude Mice and Expression of FGF2–EGFR Signaling Pathway-Related Proteins

In addition, the AI for tumor tissues of each group was measured by TUNEL detection (Figure 8A). Compared with the control group, the AI values in the miR-124-3p and sh-MGAT5 groups were dramatically increased ( $p < 0.05$ ), and the effect of miR-124-3p was weakened by

the MGAT5 mimic ( $p < 0.05$ ). Expression levels of FGF2 and p-EGFR/EGFR in tumor tissues were analyzed by Western blotting (Figure 8B and C). The expression of FGF2 and p-EGFR/EGFR in tumor tissue was decreased in the miR-124-3p and sh-MGAT5 groups compared with the control group ( $p < 0.05$ ), and increased in the miR +MGAT5 group compared with the miR-124-3p group ( $p < 0.05$ ).

## Discussion

Chemotherapy is currently the most important treatment for lung adenocarcinoma. However, owing to changes in molecular expression profiles, NSCLC is prone to primary or acquired resistance to chemotherapy regimens, resulting in poor efficacy of chemotherapy. Recently, the development of molecular targeted therapies has created new hope for patients with lung adenocarcinoma. Great progress has been made in related research, dramatically improving prognosis. EGFR is considered to be a pivotal target in biological-targeted therapies for lung adenocarcinoma. Studies have confirmed that EGFR is the driving gene of NSCLC. The detection of the EGFR gene has become an important basis for clinical treatment options in advanced

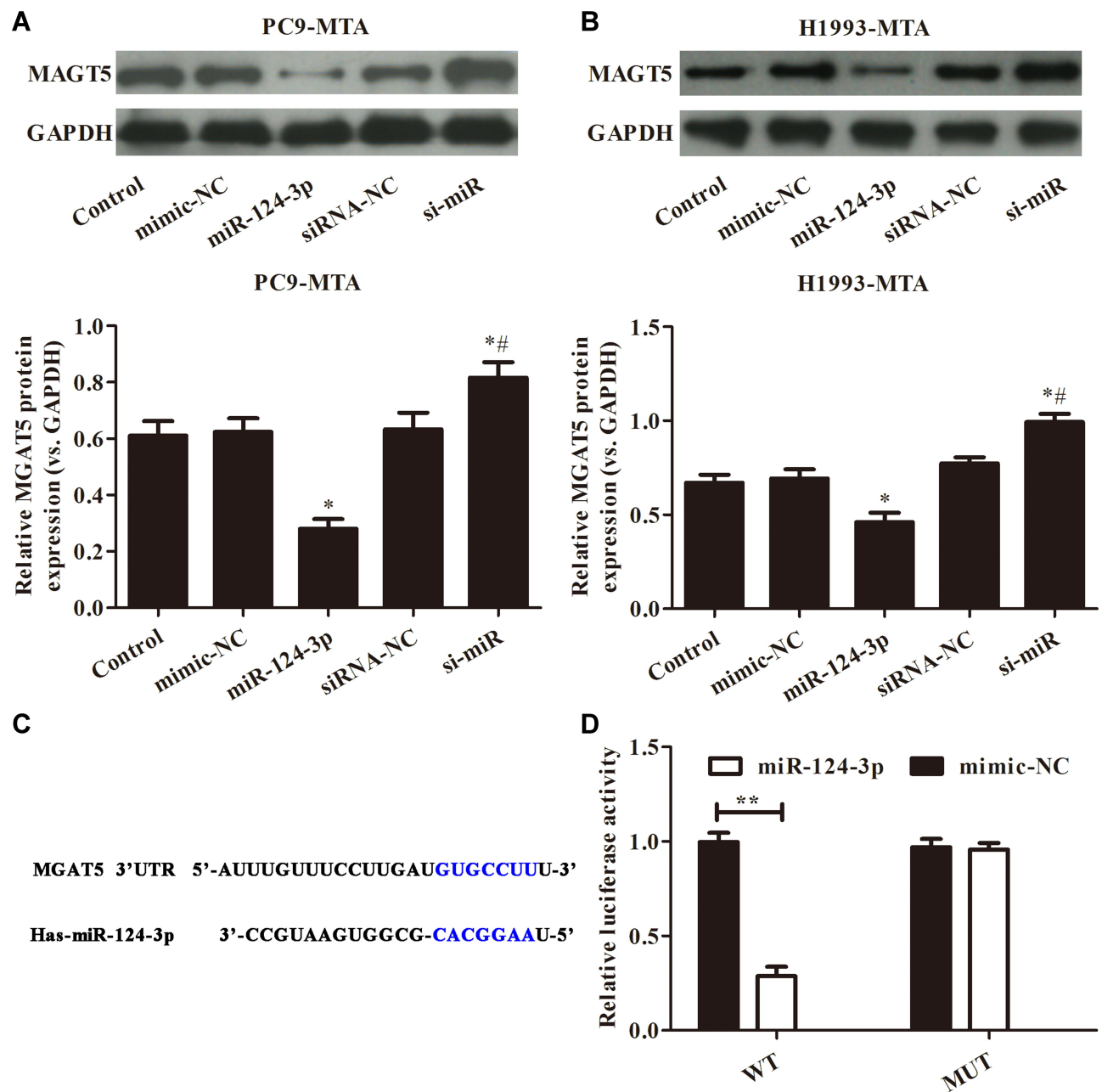


**Figure 4** Dual-luciferase reporter assay system. (A) The expression of MGAT5 protein was detected by Western blotting in PC9-MTA cells. (B) The expression of MGAT5 protein was detected by Western blotting in H1993-MTA cells. (C) Predicted binding sites of miR-124-3p and MGAT5 3'UTR by TargetScan (<http://www.targetscan.org>). (D) Dual-luciferase reporter results for recombinant vector of miR-124-3p and target gene MGAT5. \* $p < 0.05$  compared with control group; # $p < 0.05$ , \*\* $p < 0.01$  compared with miR-124-3p group.

or non-surgical NSCLC.<sup>20</sup> FGF2, also known as basic fibroblast growth factor, enhances tumorigenesis and development by regulating the transcription and translation of various genes. Recent studies have shown that FGF2 has pivotal roles in inhibiting cancer cell apoptosis and inducing chemotherapy resistance.<sup>21,22</sup> The FGF2–EGFR autocrine loop has a compensatory role in promoting the survival and growth of EGFR kinase inhibitor-resistant

cells.<sup>22</sup> In this study, changes in the FGF2–EGFR pathway were analyzed in anti-pemetrexed lung adenocarcinoma cells (PC9-MTA and H1993-MTA).

Recently, miRNAs that act as a new class of oncogenes or tumor suppressor genes were found to be closely related to the occurrence of various cancers,<sup>23</sup> triggering a worldwide research boom. Accumulating evidence indicates that dysregulation of miRNAs functions in the

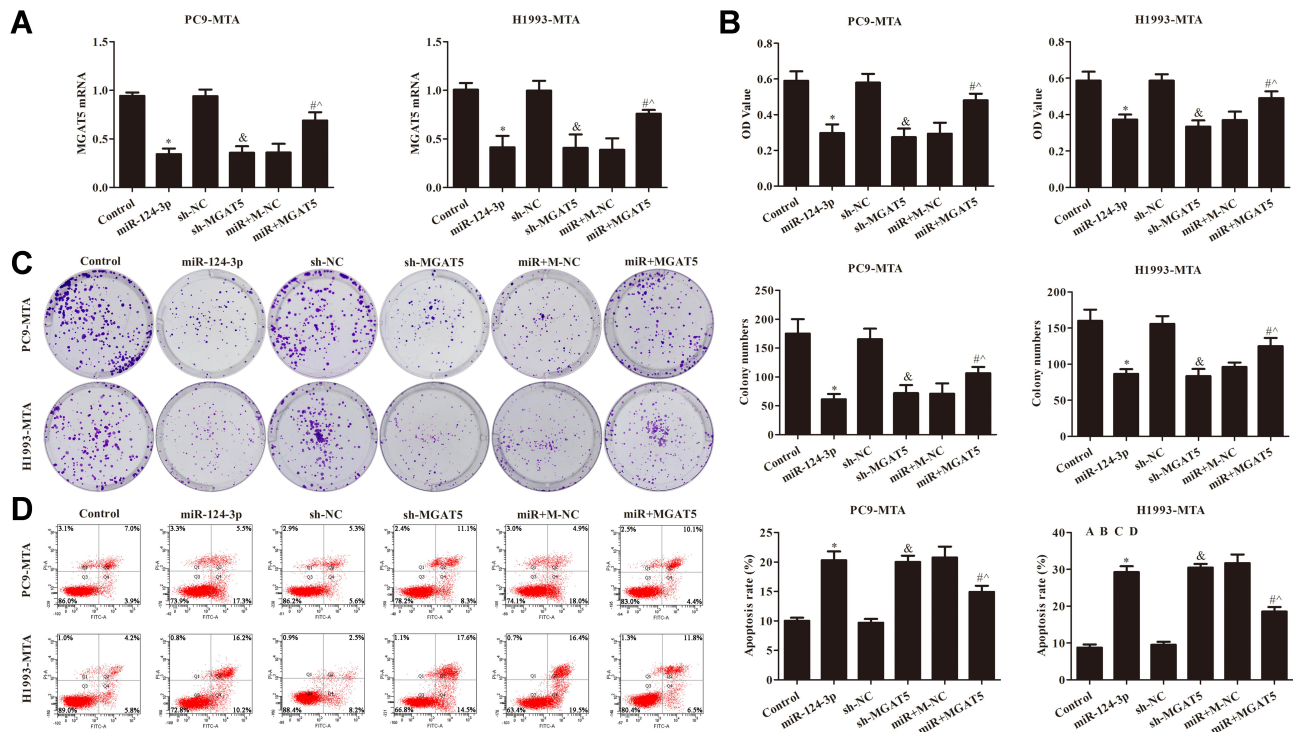


**Figure 5** Effects of miR-124-3p targeting of MGAT5 on the biological behavior of anti-pemetrexed cells. **(A)** Expression of MGAT5 mRNA detected by RT-PCR in each group. **(B)** CCK8 assay to detect cell viability. **(C)** Colony formation experiment to analyze cell proliferation. **(D)** Cell apoptosis detected by flow cytometry. Compared with control group, \* $p < 0.05$ ; compared with miR-124-3p group, # $p < 0.05$ ; compared with sh-NC group, & $p < 0.05$ ; compared with miR+M-NC group, ^ $p < 0.05$ . **Abbreviations:** miR-124-3p, miR-124-3p overexpression group; sh-NC, MGAT5 silencing negative control group; sh-MGAT5, MGAT5 silencing group; miR+M-NC group, miR-124-3p overexpression + MGAT5 overexpression negative control group; miR+MGAT5, miR-124-3p overexpression + MGAT5 overexpression group.

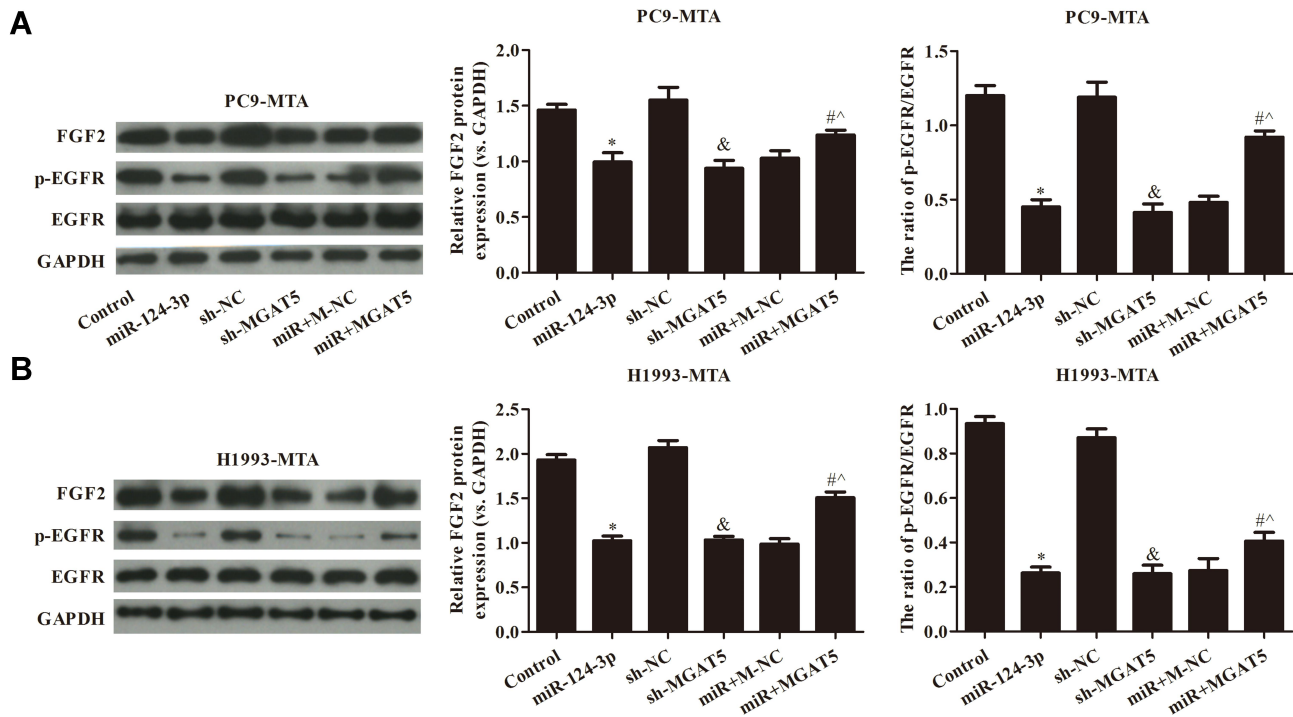


**Figure 6** Effects of miR-124-3p targeting MGAT5 on the expression of FGF2-EGFR signaling pathway-related proteins in PC9-MTA cells **(A)** and H1993-MTA cells **(B)**. \* $p < 0.05$  compared with control group; # $p < 0.05$  compared with miR-124-3p group; & $p < 0.05$  compared with sh-NC group; ^ $p < 0.05$  compared with miR+M-NC group. **Abbreviations:** miR-124-3p, miR-124-3p overexpression group; sh-NC, MGAT5 silencing negative control group; sh-MGAT5, MGAT5 silencing group; miR+M-NC group, miR-124-3p overexpression + MGAT5 overexpression negative control group; miR+MGAT5, miR-124-3p overexpression + MGAT5 overexpression group.

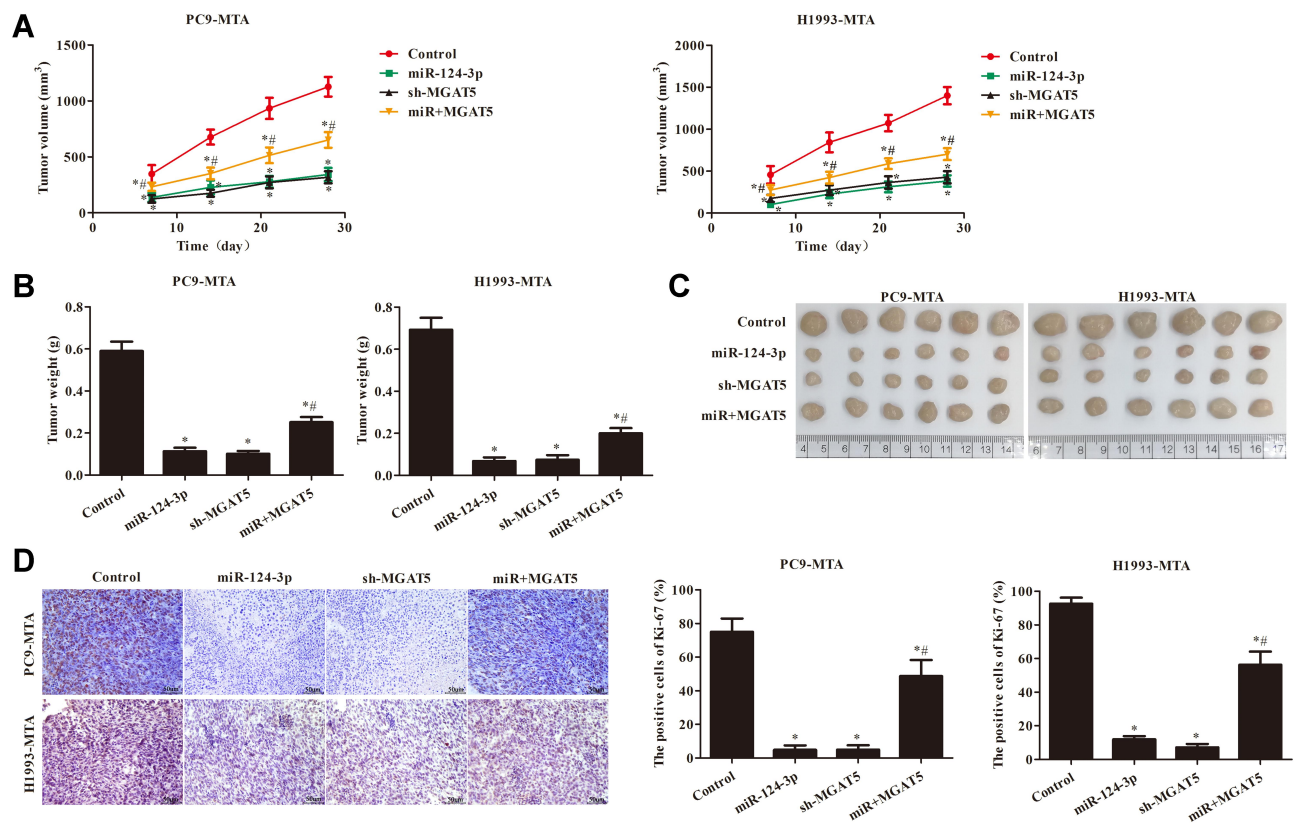


**Figure 7** Effect of miR-124-3p targeting MGAT5 on the growth of transplanted tumors in nude mice. (A) Tumor volume; (B) tumor weight; (C) tumor photographs; (D) immunohistochemical detection of Ki67 expression in transplanted tumors ( $\times 400$ ). \* $p < 0.05$  vs control group; # $p < 0.05$  vs miR-124-3p group.

**Abbreviations:** miR-124-3p, miR-124-3p overexpression group; sh-MGAT5, MGAT5 silencing group; miR+MGAT5, miR-124-3p overexpression + MGAT5 overexpression group.

initiation and progression of cancer. Studies have found that some miRNAs can play a part in the diagnosis and treatment of lung tumors or lung cancer, and can be used to reduce the symptoms.<sup>24</sup> One study found that deregulation of expression of miR-21, miR-143, and miR-181a in NSCLC, indicating that these miRNAs could be powerful tools for cancer prevention and therapeutics.<sup>25</sup> A study in 2016 found that miR-124 was significantly downregulated in lung adenocarcinoma tissue.<sup>26</sup> Zhou and colleagues found that MGAT5 was expressed at a relatively high level in CD133+ lung adenocarcinoma cells, and that it had an important role in cancer cell growth in vitro and in vivo.<sup>19</sup> However, there have been few studies on the role of miRNA-124-3p and MGAT5 in lung adenocarcinoma and its related signaling pathways.

In this work, anti-pemetrexed lung adenocarcinoma cell lines and a transplanted tumor model in nude mice were constructed to investigate whether miR-124-3p regulates the FGF2–EGFR pathway by targeting MGAT5 to affect the resistance of pemetrexed in lung adenocarcinoma cells. Preliminary results showed that the expression

of miR-124-3p in anti-pemetrexed lung adenocarcinoma cells was lower than that of the parent lung adenocarcinoma cells. Furthermore, miR-124-3p overexpression suppressed proliferation of anti-pemetrexed lung adenocarcinoma cells and inhibited FGF2 and p-EGFR expression in vitro and in vivo. The dual-luciferase reporter system further verified that MGAT5 was indeed a target of miR-124-3p. These results indicated that miR-124-3p might regulate the expression of FGF2 and p-EGFR/EGFR proteins by targeting MGAT5.

Our current data provide the mechanism of miR-124-3p in proliferation of anti-pemetrexed lung adenocarcinoma cells. However, there are many limitations to this research. The results could not fully explain the morphological differences between PC9-MTA and H1993-MTA cells, and the other mechanisms of miR-124-3p in anti-pemetrexed lung adenocarcinoma cells are still unclear.

## Conclusions

Low expression of miR-124-3p is a significant molecular event in the development of resistance to pemetrexed in

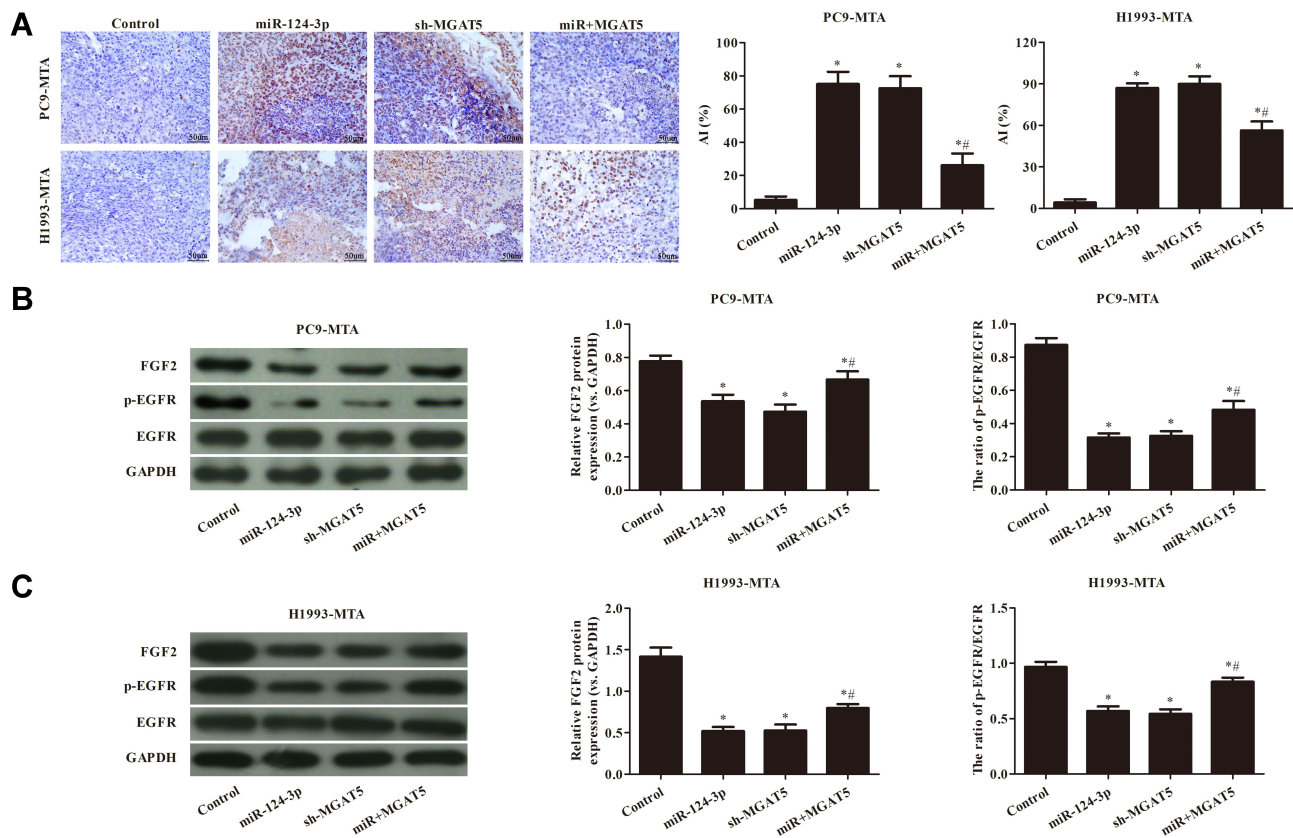


**Figure 8** Effects of miR-124-3p on apoptosis of transplanted tumors in nude mice and expression of FGF2–EGFR signaling pathway-related proteins by targeting MGAT5. (A) Tumor cell apoptosis detected using TUNEL kit (×400); (B) FGF2–EGFR signaling pathway-related protein expression in PC9-MTA tumor tissue detected by Western blot; (C) FGF2–EGFR signaling pathway-related protein expression in H1993-MTA tumor tissue detected by Western blot. \* $p < 0.05$  vs Control group; \*\* $p < 0.05$  vs miR-124-3p group.

**Abbreviations:** miR-124-3p, miR-124-3p overexpression group; sh-MGAT5, MGAT5 silencing group; miR+MGAT5, miR-124-3p overexpression + MGAT5 overexpression group.

lung adenocarcinoma cells, which is involved in tumor progression. The above results show that targeting of MGAT5 by miR-124-3p could decrease pemetrexed resistance in lung adenocarcinoma cells by inhibiting the FGF2–EGFR pathway. Therefore, miR-124-3p is a potential therapeutic target to overcome drug resistance in the treatment of lung adenocarcinoma.

## Data Sharing Statement

The datasets used and/or analysed during the current study are available from the corresponding author on reasonable request.

## Ethics Approval

Animal experiments were followed the NIH guidelines (NIH Pub. No. 85-23, revised 1996) and have been approved by the Animal Protection and Use Committee of Tianjin Medical University Cancer Institute and Hospital.

## Funding

There is no funding to report.

## Disclosure

The authors declare that they have no competing interests.

## References

1. Beasley MB, Brambilla E, Travis WD. The 2004 World Health Organization classification of lung tumors. *Semin Roentgenol.* 2005;40(2):90–97. doi:10.1053/j.ro.2005.01.001
2. Duma N, Santana-Davila R, Molina JR. Non-small cell lung cancer: epidemiology, screening, diagnosis, and treatment. *Mayo Clin Proc.* 2019;94(8):1623–1640. doi:10.1016/j.mayocp.2019.01.013
3. Siegel RL, Miller KD, Jemal A. Cancer statistics, 2016. *CA Cancer J Clin.* 2016;66(1).
4. Ettinger DS, Akerley W, Borghaei H, Chang AC, Hughes M. Non-small cell lung cancer, version 6.2015. *J Natl Compr Canc Netw.* 2013;11(6):645–653. doi:10.6004/jnccn.2013.0084
5. Ettinger DS, Akerley W, Borghaei H, et al. Non-small cell lung cancer. *J Natl Compr Canc Netw.* 2012;10:1236. doi:10.6004/jnccn.2012.0130
6. Chang A. Chemotherapy, chemoresistance and the changing treatment landscape for NSCLC. *Lung Cancer.* 2011;71(1):3–10. doi:10.1016/j.lungcan.2010.08.022

7. Scagliotti G, Hanna N, Fossella F, et al. The differential efficacy of pemetrexed according to NSCLC histology: a review of two Phase III studies. *Oncologist*. 2009;14(3):253–263. doi:10.1634/theoncologist.2008-0232
8. Ciuleanu T, Brodowicz T, Zielinski C, Kim JH, Belani CP. Maintenance pemetrexed plus best supportive care versus placebo plus best supportive care for non-small-cell lung cancer: a randomized, double-blind, Phase 3 study. *Lancet*. 2009;374(9699):1432–1440. doi:10.1016/S0140-6736(09)61497-5
9. Scagliotti GV, Ceppi P, Capelletto E, et al. Updated clinical information on multitargeted antifolates in lung cancer. *Clin Lung Cancer*. 2009;10:S35–S40. doi:10.3816/CLC.2009.s.006
10. Liu X, Ping W, Zhang C, Ma Z. Epidermal growth factor receptor (EGFR): a rising star in the era of precision medicine of lung cancer. *Oncotarget*. 2017;8(30).
11. Hanauske AR, Eismann U, Oberschmidt O, et al. In vitro chemosensitivity of freshly explanted tumor cells to pemetrexed is correlated with target gene expression. *Invest New Drugs*. 2007;25(5):417–423. doi:10.1007/s10637-007-9060-9
12. Han ZB, Zhong L, Teng MJ, et al. Identification of recurrence-related microRNAs in hepatocellular carcinoma following liver transplantation. *Mol Oncol*. 2012;6(4):445–457. doi:10.1016/j.molonc.2012.04.001
13. Liu YY, Zhang LY, Du WZ. Circular RNA circ-PVT1 contributes to paclitaxel resistance of gastric cancer cells through the regulation of ZEB1 expression by sponging miR-124-3p. *Biosci Rep*. 2019;39(12). doi:10.1042/BSR20193045
14. Hu D, Li M, Su J, Miao K, Qiu X. Dual-targeting of miR-124-3p and ABCG4 promotes sensitivity to adriamycin in breast cancer cells. *Genet Test Mol Biomarkers*. 2019;23(3):156–165. doi:10.1089/gtmb.2018.0259
15. Wang Z, Dai J, Yan J, Zhang Y, Yin Z. Targeting EZH2 as a novel therapeutic strategy for sorafenib-resistant thyroid carcinoma. *J Cell Mol Med*. 2019;23(7):4770–4778. doi:10.1111/jcmm.14365
16. Yan G, Li Y, Zhan L, et al. Decreased miR-124-3p promoted breast cancer proliferation and metastasis by targeting MGAT5. *Am J Cancer Res*. 2019;9(3):585–596.
17. Feng X, Luo Q, Wang H, Zhang H, Chen F. MicroRNA-22 suppresses cell proliferation, migration and invasion in oral squamous cell carcinoma by targeting NLRP3. *J Cell Physiol*. 2018;233(9):6705–6713. doi:10.1002/jcp.26331
18. G ML H, Dong F, Hu X, Liu S, Sun H. Inhibition of microRNA 124-3p protects against acute myocardial infarction by suppressing the apoptosis of cardiomyocytes. *Mol Med Rep*. 2019;20(4):3379–3387.
19. Zhou X, Chen H, Wang Q, Zhang L, Zhao J. Knockdown of Mgat5 inhibits CD133+ human pulmonary adenocarcinoma cell growth in vitro and in vivo. *Clin Invest Med*. 2011;34(3):155–162. doi:10.25011/cim.v34i3.15188
20. Paez JG, Jänne PA, Lee JC, et al. EGFR mutations in lung cancer: correlation with clinical response to gefitinib therapy. *Science*. 2004;304:1497–1500.
21. Turner N, Grose R. Fibroblast growth factor signalling: from development to cancer. *Nat Rev Cancer*. 2010;10(2):116–129. doi:10.1038/nrc2780
22. Miura K, Oba T, Hamanaka K, Ito KI. FGF2-FGFR1 pathway activation together with thymidylate synthase upregulation is induced in pemetrexed-resistant lung cancer cells. *Oncotarget*. 2019;10(11):1171–1192. doi:10.18632/oncotarget.26622
23. Medina PP, Slack FJ. MicroRNAs and cancer: an overview. *Cell Cycle*. 2008;7(16):2485–2492. doi:10.4161/cc.7.16.6453
24. Yanaihara N, Caplen N, Bowman E, et al. Unique microRNA molecular profiles in lung cancer diagnosis and prognosis. *Cancer Cell*. 2006;9(3):189–198. doi:10.1016/j.ccr.2006.01.025
25. Gao W, Yu Y, Cao H, et al. Deregulated expression of miR-21, miR-143 and miR-181a in non small cell lung cancer is related to clinicopathologic characteristics or patient prognosis. *Biomed Pharmacother*. 2010;64(6):0–408. doi:10.1016/j.biopha.2010.01.018
26. Wang X, Liu Y, Liu X, et al. MiR-124 inhibits cell proliferation, migration and invasion by directly targeting SOX9 in lung adenocarcinoma. *Oncol Rep*. 2016;35:3115–3121.

## Cancer Management and Research

Dovepress

### Publish your work in this journal

Cancer Management and Research is an international, peer-reviewed open access journal focusing on cancer research and the optimal use of preventative and integrated treatment interventions to achieve improved outcomes, enhanced survival and quality of life for the cancer patient.

The manuscript management system is completely online and includes a very quick and fair peer-review system, which is all easy to use. Visit <http://www.dovepress.com/testimonials.php> to read real quotes from published authors.

Submit your manuscript here: <https://www.dovepress.com/cancer-management-and-research-journal>